THERMOMECHANICAL TREATMENT OF TIAL6V4 ALLOY FABRICATED BY SELECTIVE LASER MELTING: OPTIMIZATION OF MICROSTRUCTURE AND FATIGUE PROPERTIES

Galina Kasperovich, Joachim Hausmann

Institute of Materials Research, German Aerospace Center, Cologne, Germany

Keywords: Selective laser melting, Thermomechanical treatment, Titanium alloys, Fatigue

Abstract

The ultimate goal of the research is the production of complex Ti alloy parts such as turbine blades with internal cooling channels by selective laser melting (SLM). In the first instance the possibility of a significant reduction of the porosity of TiAl6V4 parts through the optimization of process parameters is presented. This allows avoiding cracks and other types of localized irregularities of the parts. Further thermomechanical treatment of TiAl6V4 samples such as annealing and hot-isostatically pressing (HIP) changes the microstructure of the material and its static and cyclic strength drastically. Hot isostatic pressing removes residual porosity and fuses unmolten particles together significantly. The microstructure of the annealed and "HIPed" material in comparison to the non-treated alloy and to the wrought TiAl6V4 reference material is analysed. The effect of the thermomechanical treatments on the fatigue properties of TiAl6V4 specimens fabricated by SLM is presented and discussed.

Introduction

Generative processes or additive manufacturing enable the production of complex component geometries with high precision, which is difficult or impossible to realize using conventional techniques. Titanium alloys are extensively investigated and utilized in selective laser melting (SLM) processes [e.g. 1, 2, 3]. In particular, the TiAl6V4 alloy has a great potential and is widely used in aerospace industry. However, the presence of unmolten particles, which lead to cracks and other types of localized irregularities in the parts processed by SLM, and their high porosity necessitates further optimization of the production process in order to minimize possible defects. This study presents an option to significantly reduce the porosity of TiAl6V4 parts through the improvement of process parameters due to a careful analysis of the surface and volume porosities for each technology choice.

Further thermomechanical treatments such as annealing and hot isostatic pressing (HIP) change the microstructure of the SLM material and its strength and durability characteristics drastically. Tensile tests, fatigue tests and hardness measurements were used to investigate the influence of the thermomechanical treatment on mechanical properties for all investigated stages: for an optimized basic SLM structure, for the same structure after annealing and after HIP. Similar tests were also conducted for the reference material: forged TiAl6V4. Despite the fact that many research activities were performed on characterization of materials produced by SLM, there are almost no publications on fatigue resistance except Ref. [3]. Thus, the focus of this paper is the role of defects regarding fatigue properties of SLM produced parts (more details on tensile tests will be published in [4]).

Qualitative and quantitative analysis of porosity, cross microstructural characterization, investigation of fatigue fractures, cracks study by means of light optical microscopy, scanning electron microscopy and X-Ray computer tomography allowed to figure out the

microstructure-property relationship. The ultimate goal of the research is the production of complex parts, which are very costly or impossible to produce when using conventional processes. An exemplary application is a turbine blade with thin internal cooling channels. The surface of the channels cannot be machined or polished. Therefore, both treated ('machined') and untreated ('as built') surface conditions of the material need to be considered with respect to susceptibility to crack initiation. An effect of thermomechanical treatments on the properties of 'as built' and 'machined' TiAl6V4 parts fabricated by SLM will be discussed.

Material and experimental methods

Ti6Al4V powder and optimization of SLM process

For this investigation the α–β titanium alloy TiAl6V4 (Ti-6wt%Al-4wt%V) was used, which was powderised by gas atomization, resulting in spherical particles. The particles have a size distribution between 5 μm and 80 μm. 80 pct of the particle volume has a powder size smaller than 40 μm.

The microstructure evolution of a SLM part is governed by the local heat transfer conditions which are influenced by laser energy, scanning speed, spot size etc. For the optimization program more than 30 small cuboids (12 × 10 × 10 mm^3) were produced by a Concept Laser M2 (LaserCusing®) machine at the central workshop of DLR 'Systemhaus Technik' in Cologne, Germany with following process parameters:

- scanning velocity: 850, 1000, 1250 and 1500 mm/s;
- laser power: 55 %, 100 % - depending on the maximum power capacity of the machine (P_{max} = 200 W);
- spot size: small (S), medium (M) and large (L) – depending on the machine settings specific distance (from 150 up to 250 μm).

One part of all test cuboids was analyzed two-dimensionally (2D) by metallographic cross sections perpendicular to the building direction, whereas the second part was used for three-dimensional (3D) porosity investigations by computer tomography.

Before 2D microstructural examination, the samples were ground using a SiC grinding paper with up to 4000 grit sizes, and polished using a SiO_2–H_2O_2 solution. To reveal the microstructure, the polished surfaces were etched in a mixture of 50 ml distilled water, 25 ml HNO_3 and 5 ml HF [32]. The microstructural analyses were performed on a ZEISS optical light microscope and a ZEISS ULTRA 55 scanning electron microscope (SEM).

The porosity study is carried out by a comparison of the microstructures using the quantitative image analysis program AnalySIS© [31]. The surface area, perimeter, and mean diameter of each pore were determined, analyzed and classified. A statistical analysis of the results was performed. The investigated surface area was 12 × 10 mm^2 for each sample and an average of 3 different longitudinal sections was taken. The etched surfaces showed significantly greater and clearly excessive porosity, while not etched surfaces appeared to show lower values. The real porosity value is likely somewhere in-between, and, hence, porosity was determined for both conditions of the surfaces: for not etched and for etched. The porosity of the same sample differs significantly depending on the applied analysis technique (Figures 1a and 1b).

The 3D porosity was created through 3D reconstructions using X-ray phoenix nanotom® computer tomography with an acceleration voltage of 100 kV and current of 100 μA (Figure 1c). A specimen taken from the second part of the test cuboids was placed on the rotating

stage in the X-ray tomography, and the projections during rotation under X-ray radiation were collected. The pictures were segmented into binary images with datos|x-reconstraction©, the three-dimensional volume was reconstructed by VGStudioMax©, and the reconstructions were then used for the volumetric porosity calculations. The 3D porosity of two specimens for each parameter set was examined and the average was taken.

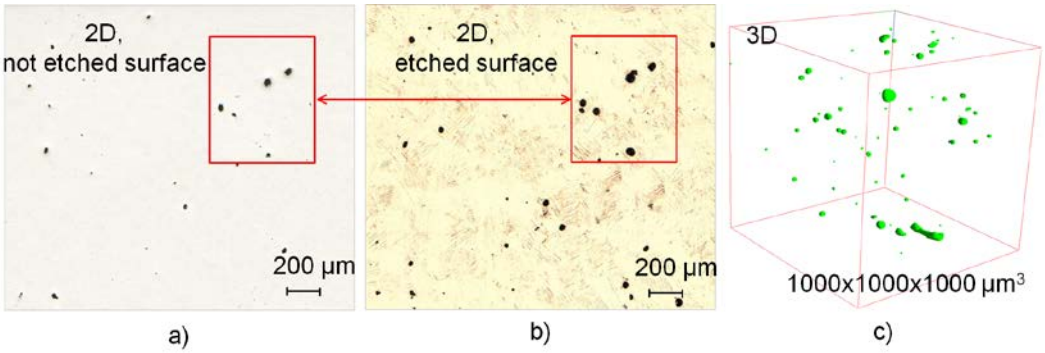

Fig. 1. Relative surface porosity values depend on the method of surface treatment: the porosity for the not etched surface is 0.1333% (a) and the same etched surface in the middle has a porosity of up to 0.5785% (b). 2D porosity values refer to the total analyzed area 12 x 10 mm^2, whose small fragments are presented here. The image (c) on the right shows an example of 3D measurement: the volume porosity is 0.4147% for the analyzed volume 1000 x 1000 x 1000 μm^3.

The 2D and 3D results were compared and analyzed. Optimal technological options were chosen based on the minimum amount of porosity.

Heat treatment and surface conditions

The optimized process parameters were subsequently used to produce cylindrical fatigue specimens to investigate the influence of thermomechanical treatment on the microstructure and the mechanical properties. More than 60 specimens with a gauge diameter of 5 mm were built vertically along their axis. A part of the specimens was tested with machined and polished surface within the gauge length while another part was tested with non-machined rough surface obtained by the SLM-process. Both ‘as built’ and ‘machined’ specimens were subjected to further thermomechanical treatment: annealing and hot-isostatically pressing (HIP). In order to obtain a good comparison with TiAl6V4 produced by traditional processes, ten tensile specimens were machined from a wrought rod for similar testing.

So, TiAl6V4 samples were investigated in the following states:

- ‘Reference’ - wrought TiAl6V4 as reference material;
- TiAl6V4 samples fabricated by SLM with optimized process parameters:
  - ‘SLM’ - without further treatment;
  - ‘SLM, heat’ - annealed at 700 °C for one hour, and then cooled with a constant cooling rate of 10 K/min;
  - ‘SLM, HIP’ - hot-isostatically pressed (HIP) at 910 °C and 100 MPa for two hours at an argon atmosphere, subsequently annealed at 700 °C for one hour and then cooled with a constant cooling rate of 10 K/min.

Mechanical testing

Vickers microhardness tests were performed on an automated CLEMEX microhardness tester using a weight of 100 g. For each sample, an average of 100 measurements was given.

Fatigue tests were subjected to uniaxial sinusoidal cyclic loading with a stress ratio of R = - 1, a test frequency of f = 80 Hz and at a stress amplitude of 600 MPa. All experiments were carried out at room temperature. SLM HIP material has been more widely studied by HCF with σ_{max} = 200, 350 and 500 MPa under fully reversed loading (R = - 1).

Energy dispersive X-ray (EDS) element analysis was carried out with an Oxford spectrometer (Oxford Instruments, High Wycombe, UK) attached to the SEM. For detailed study of structure and phase composition X-Ray diffraction (XRD) was performed. XRD data were obtained on a SIEMENS-D5000 diffractometer. $CuK_{\alpha 1}$ radiation was used. Reflections in the 2θ range 20 - 100° were recorded.

Results and Discussion

Process optimisation – porosity study

The optimization process was carried out with a careful analysis of the 2D and 3D porosity of the test samples for each set of parameters.

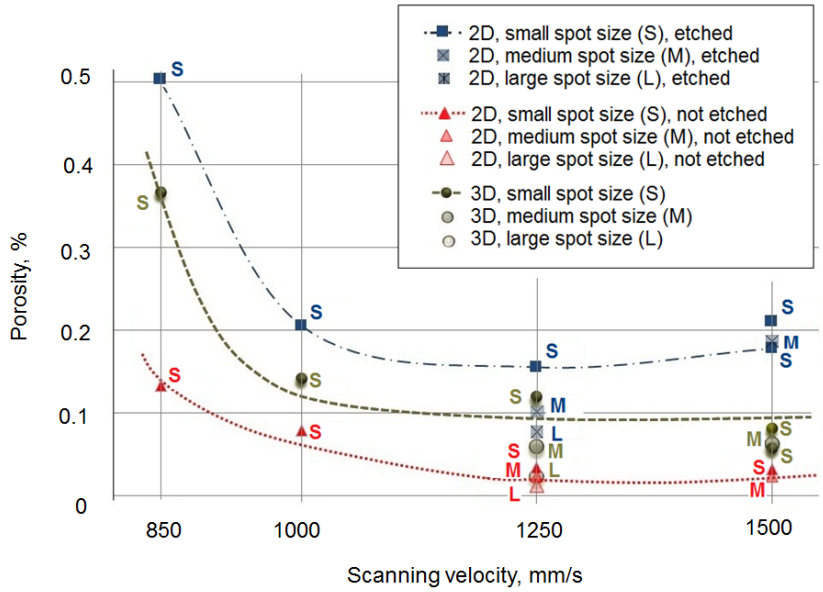

Fig. 2. The 2D and 3D measured porosity of the test samples, obtained at different process parameters (laser power 100 %).

As expected, cross section-analyzed samples that were not treated with an etchant (Figure 2, red dotted trace) show a smaller numerical value of the porosity than etched samples (Figure 2, blue curve). This can be explained on the one hand with a size expansion of the pores by the etchant, whereas on the other hand small pores may be closed by smeared material on the untreated specimens. A better approximation to the real porosity is most likely obtained from the 3D tomographic measurement (Figure 2, green broken curve). In order to avoid errors from artifact phenomena in the tomographic scan, pores detected with sizes below 4 µm in mean diameter were not considered due to the limited resolution of 1.2 µm/voxel. Thus, it can be assumed that the real value of porosity will be between the 2D etched and the 3D values.

Despite the differences caused by the different measurement techniques (2D for the etched, and not-etched surfaces and 3D), the tendency of the porosity is the same in all cases. With the increase of the scanning velocity up to 1250 mm/s the porosity reduces considerably. However, a further increase does not decrease the porosity anymore. Contrary, the porosity increases due to appearance of a large number of small pores of less than 4 microns, which were not taken into account in 3D analysis. Therefore, some values of 3D porosity at the high scanning velocity show no increase (for example, increased 3D value for the small spot size

at 1500 mm/s: 80 % of the pores in this case have a diameter smaller than 4 µm as shown in the Figure 3). The spot sizes ('S', 'M' or 'L' in the Figure 2) are essential for minimizing the porosity. Larger spot sizes are preferable. A similar trend was also obtained with a laser power of 55 %. A slightly higher value of porosity was received in this case.

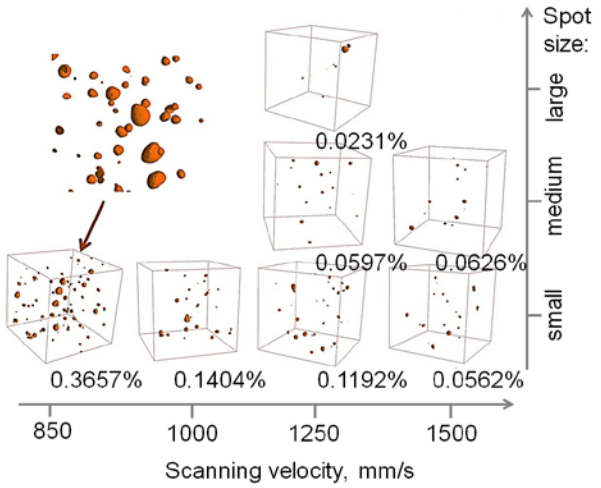

Fig. 3. Example of 3D porosity study: pores in the test samples produced with different technological parameters: scanning velocity (changes from left to right) and spot size (changes from the bottom to the top). The volumes here are 1000 x 1000 x 1000 µm^3. TiAl6V4 phase is transparent.

The lowest values of porosity were determined for the following process parameters: scanning speed of 1250 mm/s, large spot size at 100% laser power – 0.023 % (for the etched surface). Therefore, these parameters were chosen for manufacturing the specimens.

Porosity study was also presented for the post heat-treated specimens and for the specimen after HIP. As expected heat treatment does not show significant influence on porosity, while the HIP considerably reduces it: after the HIP process the 2D porosity of the sample was less than 0.012 % (for the etched surface).

Effect of thermomechanical treatment on the microstructure and the fatigue properties

The microstructure of the TiAl6V4 alloy can be lamellar or globular depending on the rate of solidification. The lamellar microstructure is usually preferable for fracture toughness, fatigue crack propagation and oxidation behavior, whilst the globular microstructure is better for strength, ductility and fatigue crack initiation. Conventional microstructure of TiAl6V4 can be fundamentally classified by the size and the arrangement of the two phases α (hcp) and β (bcc) [5]. The microstructure of the wrought material is shown in Figure 4 ('Reference'), where an α-globular phase in an α + β matrix is observable. The presence of the β-phase (8.6%) is confirmed by XRD analysis.

The fast cooling rate during the SLM process results in an acicular martensitic phase or the α´ phase, which is hexagonally packed (Figure 4, 'SLM' sample). Due to partial remelting of the previous layers, elongated α´ grains grow up to several tens of micrometers in length that can be observed by XRD. The XRD diffraction patterns indicate the presence of a hexagonal phase with lattice parameters a = 0.29231 nm and c = 0.466175 nm. These values correspond well to the lattice parameters values for the α´ phase, i.e. a = 0.29313 nm and c = 0.46813 nm [2, 5]. The XRD measurements do not indicate the presence of a β phase.

By the heat treating at intermediate temperatures below the β transus (700° C, 1h), the initial fine martensitic structure has been transformed into a mixture of α and β, in which the α phase is present as fine needles. A coarsening of the microstructure (s. Figure 4, 'SLM, heat' sample) is observed: the column width after the heating is a little bit higher - up to 2 µm.

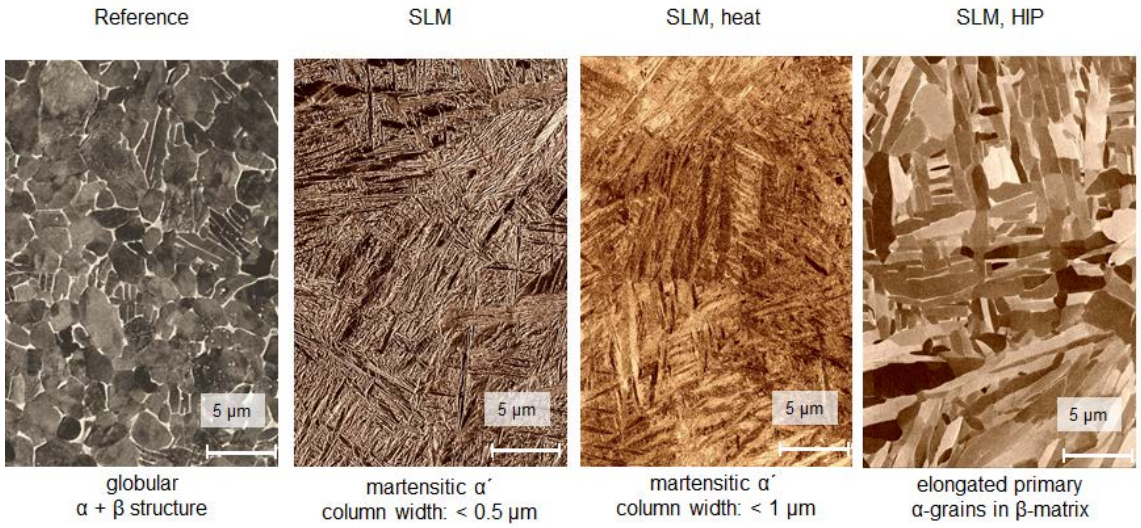

Fig. 4. Globular ('Reference') and lamellar ('SLM') structures of TiAl6V4 alloy and an effect of thermomechanical treatment on the microstructure of the SLM samples ('SLM, heat' and 'SLM, HIP'). All pictures are SEM micrographs with etched surfaces.

HIP creates a microstructure that represents the elongated α grains embedded in β-phase grain boundaries (Figure 4, 'SLM, HIP' sample): column width: 2 - 3 µm, length up to 50-60 µm. The XRD diffraction patterns indicate the presence of a duplex α/β structure in the HIP samples with lattice parameters a = 0.292337 nm and c = 0.466731 nm for α-Ti and with a = 0.31948 for β-Ti.

The Vickers microhardness tests show higher values for the samples with the martensitic structure (360 for the 'SLM' and 351 for the 'SLM, heat') in comparison to the 'Reference' and 'SLM, HIP' (314 and 321 respectively) materials as expected by the type of the microstructures. After HIP, the hardness values are almost restored to those of the reference material.

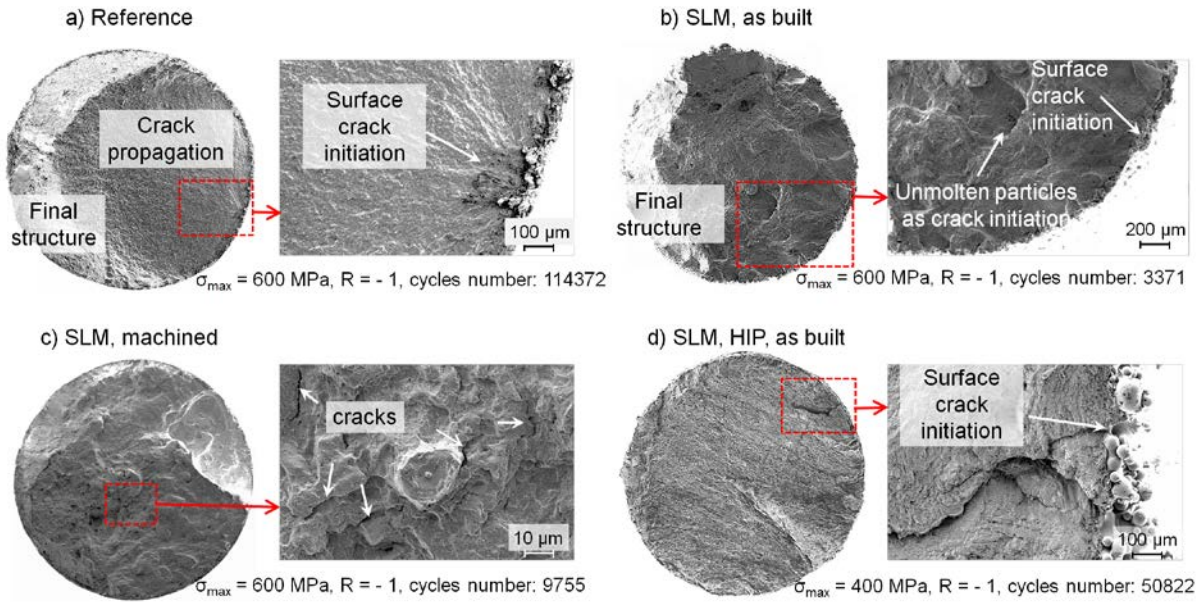

Fig. 5. Typical fracture surfaces of 'Reference' (a), 'SLM, as built' (b), 'SLM, machined' (c) and 'as built' 'SLM, HIP'(d), samples by HCF tests.

The process of fatigue failure is characterized by crack initiation, crack propagation and final failure. Cracks usually initiate on the areas with the highest stress concentration. These may be caused by notches, irregularities, cracks or pores. For the SLM fatigue specimens without machined surface ('as built'), it was found that fatigue crack initiation generally occurred at the rough surface. The fracture extended to the whole cross section and finally the specimen failed (Figure 5).

The main objective of conducting fatigue experiments in the HCF regime was to evaluate the effects of a heat treatment on the fatigue strength of SLM-processed material. The results of the HCF fatigue tests clearly showed that a heat-treatment and especially HIP had a strong impact on the fatigue behaviour (Figure 6). The rough 'as built' surface provides many micro notches which promote the initiation of cracks. From SEM images of cross sections made close to the surface of a fatigued specimen, it can be seen that the valleys of the roughness profile are preferred locations for crack initiation (more details in [4]).

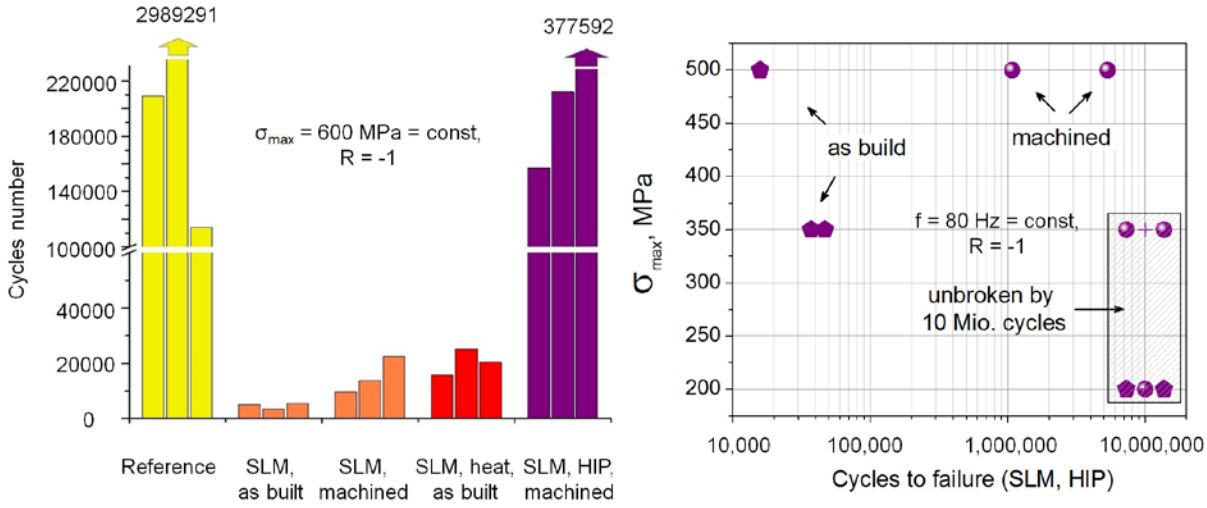

Fig. 6. Comparative analysis of the fatigue properties of TiAl6V4: 'Reference' and 'SLM', 'SLM, heat' and 'SLM, HIP', samples at a constant stress amplitude of 600 MPa (left) and fatigue testing of 'SLM, HIP' for the 'as built' and 'machined' samples by HCF with σ_{max} = 200, 350 and 500 MPa (on the right).

HIP treatment removes unmolten particles and cold joints, adjusts the microstructure, and, as a result, provides ductile fracture behavior and restores the fatigue strength, which is comparable to the 'Reference' sample (Figures 5a and 5d). The mean fatigue life of SLM samples ranges from 10000 to 20000 cycles to failure for the 'as built' and 'machined' SLM and up to 30000 cycles for the heat-treated samples, while inferior fatigue lives are observed for the reference range from 120000 cycles and more. HIP significantly increases the fatigue live of samples: it increases the number of cycles by 150000 and above (Figure 6, left).

The conclusion from these fatigue tests is that HIP is able and necessary to recover the fatigue live of SLM samples comparable to the reference material. However, we need to remark that the good fatigue properties can be obtained with 'machined' surfaces only; the crack initiation by the 'as built' surface dominates the fatigue behavior (Figure 6, on the right).

The optimized process parameters allow the manufacturing of hollow turbine blades (details in [4]). The tolerances of the final geometry (after HIP) are below 0.1 mm and no cracks are visible, 3D measured porosity was 0.0579 %. Therefore, the optimized process parameters and subsequently HIP will be used for future component manufacturing.

Conclusion

Selective laser melting (SLM) is a very powerful tool to generate geometrically complex structures of high performance materials. This renders it very interesting for aerospace industry. Titanium alloys are suited well for processing by SLM; but are prone to the formation of inner defects: pores, unmolten particles or internal cracks. Therefore, a careful optimization procedure of the process parameters is necessary to obtain a high quality material: firstly, optimization of the initial parameters for minimization of inherent defects, and secondly, optimization of the further thermomechanical treatment to minimize internal stresses and adjust the microstructure. The major goal of the present study was the evaluation of the effect of thermomechanical treatments on the properties of 'as-built' and 'machined' TiAl6V4 components fabricated by SLM. The findings lead to the following conclusions:

1. For minimizing the pore content, a high but not too high scanning velocity is preferable. Upon increasing the scanning velocity from 600 mm/s up to 1250 mm/s a sharp decrease of the porosity was observed, whereas at larger velocities the porosity slowly increases due to the high number of small pores (< 4 µm). The spot size of the laser should not be too small. The optimized parameters yield intermediate porosities below 0.025 %.
2. Hot isostatic pressing (HIP) removes residual porosity and fuses unmolten particles and kissing bonds. The microstructure and fatigue resistance of the HIP material is much closer to the wrought TiAl6V4 in comparison to the non-HIP alloy.
3. Pores have a drastic influence on the fatigue behavior of SLM- processed TiAl6V4 in the high cycle fatigue regime. A significant extension of the crack initiation phase can only be achieved by reducing the porosity. Heat treatment does not change the porosity and, thus, does not improve the durability. In contrast, HIP leads to a significant improvement of fatigue strength towards that of conventionally processed TiAl6V4.
4. For components that cannot be machined at all surfaces, the rough 'as built' surface needs to be considered as crack initiator in the design process and its lower fatigue strength has to be taken into account.
5. The application of the optimized process parameters to component manufacturing is verified by prototypes of hollow turbine blades. The tolerances of the final geometry are below 0.1 mm and no cracks are visible, the 3D measured porosity is below 0.06%. Turbine blades with high quality material and high precision have been produced

Reference

1. T. Vilaro, C. Colin and J.D. Bartout, "As-Fabricated and Heat-Treated Microstructures of the Ti-6Al-4V Alloy Processed by Selective Laser Melting". *Metall. Mater. Trans.,* A 42A (2011) 3190-3199.
2. L. Thijs, F. Verhaeghe, T. Craeghs, J. Van Humbeeck, and J.-P. Kruth, "A Study of the Microstructural Evolution During Selective Laser Melting of Ti-6Al-4V," *Acta Materialia,* Vol. 58:9, (2010), 3303-3312.
3. S. Leuders, M. Thöne, A. Riemer, T. Niendorf, T. Tröster, H.A. Richard, H.J. Maier, "On the mechanical behaviour of titanium alloy TiAl6V4 manufactured by selective laser melting: Fatigue resistance and crack growth performance", *Int. Journal of Fatigue,* 48 (2013), 300–307.
4. J. Hausmann, G. Kasperovich, "Improvement of fatigue resistance and ductility of selectively laser molten TiAl6V4", submitted in *Metall. Mater. Trans., A,* (2013).
5. Leyens, C. and Peters, M. (2003), Titanium and Titanium Alloys, Wiley-Vch Verlag GmbH & Co. KGaA, Weinheim.